

Lunar subsurface investigated from correlation of seismic noise

E. Larose,¹ A. Khan,² Y. Nakamura,³ and M. Campillo¹

Received 17 May 2005; revised 17 July 2005; accepted 22 July 2005; published 16 August 2005.

Citation: Larose, E., A. Khan, Y. Nakamura, and M. Campillo (2005), Lunar subsurface investigated from correlation of seismic noise, *Geophys. Res. Lett.*, 32, L16201, doi:10.1029/2005GL023518.

[1] By correlating seismic noise recorded by four sensors placed on the Moon during the Apollo 17 mission, we have retrieved a well-defined dispersed Rayleigh wave pulse. Inversion of its group velocity provides new constraints on the lunar subsurface structure. The estimated “signal-to-noise” ratio (SNR) of the retrieved Rayleigh wave train is strongly dependent on solar illumination, effectively making solar heating a source of seismic noise on the Moon. This result suggests that in future planetary missions it is feasible to extract information on the internal structure of extraterrestrial objects by correlating seismic noise even when natural quakes are absent.

[2] The passive imaging technique is based on the time-domain cross-correlation of acoustic or seismic waves acquired at two passive sensors. The main assumption is that the cross-correlation yields the Green function (GF) between the receivers, i.e. the impulse response recorded at one sensor, with the other acting as source. Initial applications of the method include helioseismology, where it provided images of the Sun’s interior [Duvall *et al.*, 1993] and more recently, it has been tested in the ultrasonic domain using diffuse fields [Lobkis and Weaver, 2001; Derode *et al.*, 2003; Larose *et al.*, 2004] as well as with noise [Weaver and Lobkis, 2001]. Passive imaging has also been achieved using seismic coda [Campillo and Paul, 2003] as well as seismic noise [Shapiro and Campillo, 2004; Shapiro *et al.*, 2005; Sabra *et al.*, 2005] for frequencies ranging from 0.025 to 0.2 Hz. In the latter application it provided well-resolved images of the first 20 km of the subsurface beneath California. On Earth, these studies have shown that a statistical treatment of seismic noise yield the GF when averaged over sufficiently long time. Microseismic background noise is mainly excited by surface sources like oceanic and atmospheric perturbations [Rhie and Romanowicz, 2004]. The purpose of the present paper is to take the passive imaging method beyond the Earth and apply it to extraterrestrial planets on which neither an ocean nor an atmosphere exists. In particular, our aim is to investigate the method in the case where the

microseismic background noise is made of fully diffusive waves, at frequencies higher than previously investigated [Shapiro *et al.*, 2005].

[3] The only solar system body other than the Earth from which we have seismic observations pertinent to its interior properties is the Moon. From 1969 to 1972 the US Apollo program installed one short-lived and four long-lived seismic stations on the Moon. All but the first station were operated until 1977. The data collected by the Apollo seismic network provided the basis for a number of studies of lunar seismicity and internal structure published during the 1970s, early 1980s, and again recently [Latham *et al.*, 1973; Toksöz *et al.*, 1974; Nakamura *et al.*, 1982; Khan and Mosegaard, 2002; Lognonné *et al.*, 2003]. In addition to the above passive seismic experiment, active seismic experiments were also carried out on missions 14, 16 and 17. The main objective was to infer the velocity structure of the uppermost part of the crust down to a few km depth using traditional seismic refraction techniques [Cooper and Kovach, 1974].

[4] Apollo 17 touched down on the floor of the Taurus-Littrow Valley near the southeastern rim of the Serenitatis Basin, which consists of irregular, heavily cratered regolith developed on lava flows partly filling an embayment between massifs 2 km high [Heiken *et al.*, 1991]. The Apollo 17 Lunar Seismic Profiling Experiment (LSPE) was deployed on Dec. 14, 1972 at a distance of about 180 m W-NW of the lunar module. Four geophones, with natural resonant frequencies of 7.5 Hz, here labeled G1 to G4, were deployed in a triangular array (Figure 1) and recorded the vertical ground velocity in the frequency range from 3 to 30 Hz during the landing mission in 1972 [Kovach *et al.*, 1973] and then again from August 1976 to April 1977. The geophones were simultaneously connected to the central station where the seismic signals $S_{1..4}(t)$ were sampled at 118 Hz and digitized before being telemetered to the Earth. Prior to conversion into a 7-bit digital format (counts 0 to 127), the signals were conditioned using a logarithmic compression, which was done to increase the dynamic range. A typical four-channel record is displayed in Figure 1.

[5] We processed continuous data from Aug. 15, 1976 to Apr. 24, 1977. They are time-windowed into 2016 record samples, each lasting about $T = 3$ hours for a given record d . The correlated traces are calculated directly from the raw data without applying any decompression or correction filter. The absence of decompression tends to equalize the noise amplitude. For a given pair of geophones i, j , and the record d , a cross-correlated trace is determined as:

$$C_{ij}^d(\tau) = \int_d^{d+T} S_i(t + \tau) S_j(t) dt \quad (1)$$

[6] Correlated traces are then filtered in the frequency range of interest (4–12 Hz). The central part of each trace

¹Laboratoire de Géophysique Interne et Tectonophysique (LGIT), Grenoble, France.

²Niels Bohr Institute, University of Copenhagen, Copenhagen, Denmark.

³Institute for Geophysics, John A. and Katherine G. Jackson School of Geosciences, University of Texas at Austin, Austin, Texas, USA.

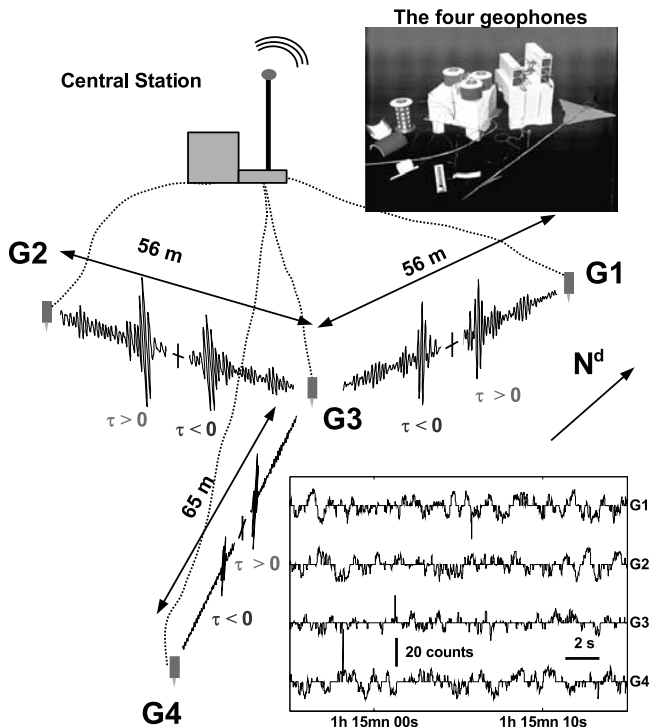


Figure 1. Configuration of the Apollo 17 LSPE experiment. It was composed of four geophones (velocimeters): G1, G2, G3 and G4, all connected to a central station for signal sampling, digitization and telemetering. A sample of raw seismic data from each geophone on Aug. 16, 1976 (UTC time) is displayed in the enclosed box (no logarithmic decompression). Typical correlations $C_{13}(\tau)$, $C_{23}(\tau)$, $C_{34}(\tau)$ are plotted between the corresponding pair of sensors. Crosses in the center of each correlation trace mark $\tau = 0$. NASA photo A17.S72_37259. See color version of this figure in the HTML.

$|\tau| < 0.5$ s (cross-talking between geophones induces a peak at the correlation time $\tau = 0$) is not displayed. Each trace is normalized by its maximum value. At the end we computed the average of the correlations over the set of records d . Typical results are displayed in Figures 1, 2a, and 3a. A well-defined pulse is observed both for positive and negative correlation times τ . Why should this pulse emerge from the correlations? Seismic waves propagating in the direction $j \rightarrow i$ add up coherently in the correlation, and contribute to this well-defined pulse for times $\tau > 0$ (causal part of the correlations). Seismic waves propagating in the opposite direction ($i \rightarrow j$) contribute to the well defined pulse for times $\tau < 0$ (acausal part of the correlations). Waves propagating in other directions add up incoherently and contribute to the residual fluctuations in the correlations [Roux *et al.*, 2004].

[7] The reconstructed pulses are interpreted as Rayleigh waves between geophones i and j , i.e. the ground velocity response of the subsurface at j to a vertical impulsive force at i . They are found to propagate with an average velocity of ~ 50 m/s, and are clearly dispersive, as shown in Figure 2a. The group velocity is evaluated by picking the envelope arrival time of the Rayleigh pulse. This pulse is filtered around 14 different frequencies, ranging from 3.6 Hz to 11.4 Hz (33% bandwidth). Velocities were calculated when

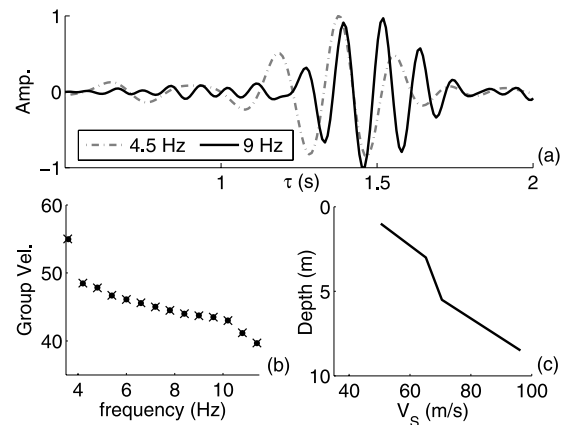


Figure 2. Dispersion analysis of the Rayleigh pulse. (a) The wave packet is filtered in two non-overlapping frequency bands (around 4.5 Hz and 9 Hz). (b) Observed dispersion curve of the Rayleigh wave group velocity. Dots: observations. Crosses: calculated data from the profile shown in (c). (c) Result of the inversion of the dispersion curve showing the upper 10 m of the shear wave velocity profile. See color version of this figure in the HTML.

the signal-to-noise ratio (SNR) of the correlated traces is > 2 . When possible we averaged velocities over the three central pairs of geophones. The group velocity dispersion curve is plotted (dots) in Figure 2b. The uncertainties on observed velocities are estimated to be 5%. This dispersion curve is used to retrieve the *shear velocity profile* through iterative linearized inversion [Herrmann and Ammon, 2004]. A four layer model was assumed with variable thickness and velocities. The inverted shear-wave velocity profile is displayed in Figure 2c. The inversion was stopped once calculated data (Figure 2b, crosses) fit the observations (dots) within 3%. While obviously more complex models can be found, our chosen parameterisation reflects the

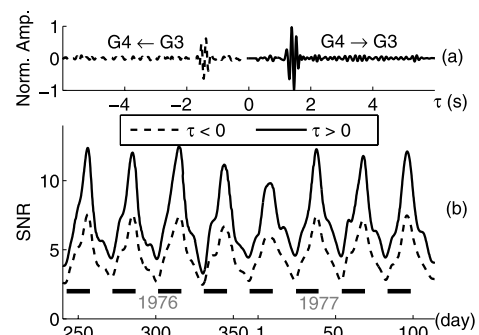


Figure 3. (a) Example of correlation $C_{34}(\tau)$ filtered in the 4–12 Hz range. The right peak (causal part, $\tau > 0$) corresponds to the Rayleigh wave propagating from G4 to G3 as if G4 was a vertical impulsive source. The left peak is the acausal part, $\tau < 0$. (b) SNR of the (right) causal and (left) acausal Rayleigh pulse as a function of record date d (x-axis in Julian days from 1976 to 1977). Thick lines represent days when the Sun was shining and heating the Apollo 17 landing site. The increase in the SNR is synchronized with the Sun's illumination, oscillating with a periodicity of 29.5 days. See color version of this figure in the HTML.

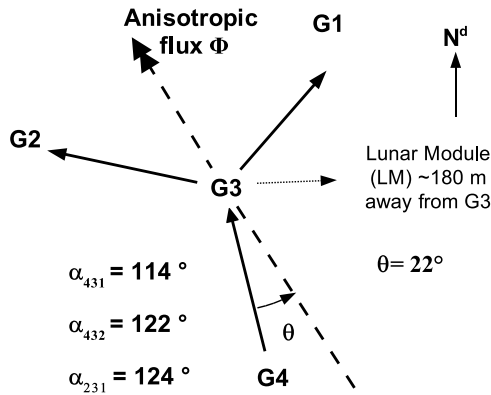


Figure 4. Schematic view of the anisotropic flux.

minimum number of layers that were found needed to fit data. The velocity jump below 5 m depth is interpreted as the base of the lunar regolith, consisting of impact breccias. *Cooper et al.* [1974], using travel time inversion of refracted P-waves, found that the *compressional wave velocity* beneath the Apollo 17 site was around 100 m/s from 0 to 4 m depth and 327 m/s from 4 to 32 m depth. Our shear wave profile thus complements their P-wave profile, giving the v_p/v_s ratio of the Lunar regolith at this site of ~ 2 . The present result is also consistent with the S-wave velocity profiles derived from the H/V spectral amplitude ratios at other Apollo sites [*Horvath et al.*, 1980], where they generally increase from 40 m/s at the surface to about 400 m/s at depths between 95 and 160 m.

[8] As a curious feature of our correlations we found that the Rayleigh wave emergence is fluctuating with time of the year. To quantify these variations, we estimated the SNR of the correlated traces as a function of record date d . The signal level corresponds to the amplitude of the (causal or acausal) peak. The noise is defined as the standard deviation of the subsequent fluctuations from $\tau = \pm 2$ s to $\tau = \pm 4$ s (Figure 3a). The SNR displayed in Figure 3b is calculated for both the causal (red) and acausal (blue) part of the correlation. It is found to fluctuate with a periodicity of exactly 29.5 days which is also the lunation period. The SNR increases during daytime (displayed as thick horizontal bars on Figure 3b) and decreases at night, pointing to an origin of the Rayleigh wave with solar illumination. When the sun heats the lunar surface, temperature increases from -170°C to $+110^\circ\text{C}$ [*Langseth et al.*, 1973], leading to very high vertical thermal gradients, and resulting in cracking of the lunar surface material and Rayleigh wave generation. This interpretation is in line with what was observed during the Apollo era where a large percentage of the seismic events were found to be very small moonquakes, termed thermal moonquakes, occurring with great regularity [*Duenneber and Sutton*, 1974]. Their activity starts abruptly about 2 days after lunar sunrise and decreases rapidly after sunset, following essentially the same trend as the SNR we observed. Thus it is most likely that the signal we observed here is derived from thermal moonquakes.

[9] The correlated traces displayed in Figures 1 and 3a are not found to be symmetric in time. Though the pulse arrival times are symmetric, waveform amplitudes may change due to preferential direction of propagation of the incident wave field [*van Tiggelen*, 2003; *Paul et al.*, 2005].

The peak amplitude for each part of the correlations, and for each couple of geophones, is evaluated. Since the reconstructed peak amplitude is proportional to the intensity of the incident waves, we interpret this asymmetry as an anisotropy of the wave field. Let us assume that the symmetric part of the traces is generated by an isotropic flux Φ_0 (waves coming from all directions onto the array), and furthermore that the asymmetric part, corresponding to the excess of amplitude observed on one part of the traces, is generated by an anisotropic flux Φ (preferential wave incidence). The peak amplitude is therefore proportional to $\Phi_0 \pm \frac{1}{2}\Phi \cos(\theta_i)$ where θ_i is the incident angle of the anisotropic flux onto the pair $i - 3$ (Figure 4). To quantify the asymmetry, we estimate the following ratio:

$$\frac{P_{3i}^+ - P_{3i}^-}{P_{3i}^+ + P_{3i}^-} = \frac{\Phi}{\Phi_0} \cos(\theta_i)$$

where P_{3i}^+ is the peak amplitude of the $C_{3i}(\tau)$ positive part. Note that this ratio for pair 3–4 can be deduced from Figure 3a. It should be noted that this flux is not a remnant wave train (which would appear as a peak at different times τ in the three pairs). It corresponds to the preferential direction of propagation of the diffuse field intensity. Using this array technique, we evaluated quantitatively the incident direction of the seismic anisotropic flux to be $+22^\circ$ relatively to $G4-G3$ (Figure 4), pointing in the S-E direction to Steno crater, as either a dense area of scatterers or an area with intense thermal moonquake activity.

[10] We have presented a technique to investigate the subsurface between passive geophones based on the correlation of lunar seismic noise. We have shown that even in a quiet seismic environment with feeble sources, it is possible to obtain a Rayleigh wave dispersion curve. From the inversion of this dispersion curve we estimated the shear wave velocity profile, which provided new information on the velocity structure of the regolith at the Apollo 17 site. Moreover, we have established the Sun as an active generator of lunar seismic noise. In particular the SNR of the reconstructed Rayleigh pulse was found to be strongly dependent on solar illumination. The seismic activity originates from the strong thermal gradients induced during lunar day as well as night. We have applied an array technique for locating noise sources. The weak anisotropy of the seismic diffuse waves reveals a preferential direction of propagation, possibly originating from an area with dense scatterers or increased thermo-seismic activity.

[11] The results presented here establish the method of extracting the Rayleigh-wave GF by cross-correlating seismic noise, as indeed extendable to extraterrestrial planets that not only differ in size, evolution and consequently seismic activity, but also in nature of origin of the noise from that of the Earth. This provides a novel avenue for future seismic exploration of the planets on which quakes might occur infrequently and are most probably also inhomogeneously distributed, of which Mars might be cited as an example [*Golombek et al.*, 1992]. In addition it holds the potential of increasing the scientific return, as noise between events can be successfully used rather than being discarded as has traditionally been the case. Specifically, to probe deeper into the subsurface on future seismic missions, the following points should be kept in mind. Distances between

stations should preferably be between one and a few tens of wavelengths, as scattering attenuation might become important for greater distances. The depth probed being roughly 1/3 of the Rayleigh wavelength, this implies going to lower frequencies which necessitates the deployment of broad-band seismometers [e.g., Lognonné *et al.*, 2000].

[12] **Acknowledgments.** The authors wish to thank A. Paul and F. Touverot for technical help, R. Weaver, N. Shapiro, L. Stehly, A. Derode and the LOA team for scientific advice. The CNRS GdR ImCODE has strongly encouraged this work. A. Khan acknowledges support from the Carlsberg Foundation, and Y. Nakamura from NASA grant NNG04GG62G.

References

- Campillo, M., and A. Paul (2003), Long range correlations in the diffuse seismic coda, *Science*, *299*, 547–549.
- Cooper, M. R., and R. L. Kovach (1974), Lunar near surface structure, *Rev. Geophys.*, *12*, 291–308.
- Derode, A., E. Larose, M. Tanter, J. de Rosny, A. Tourin, M. Campillo, and M. Fink (2003), Recovering the Green's function from field-field correlations in an open scattering medium, *J. Acoust. Soc. Am.*, *113*, 2973–2976.
- Duennebier, F., and G. H. Sutton (1974), Thermal moonquakes, *J. Geophys. Res.*, *79*, 4351–4363.
- Duvall, T., S. Jefferies, J. Harvey, and M. Pomerantz (1993), Time distance helioseismology, *Nature*, *362*, 430–432.
- Golombek, M. P., W. B. Banerdt, K. L. Tanaka, and D. M. Trally (1992), A prediction of Mars seismicity from surface faulting, *Science*, *258*, 979–981.
- Heiken, G., D. Vanniman, and B. French (1991), *Lunar Sourcebook—Users Guide to the Moon*, Cambridge Univ. Press, New York.
- Herrmann, R. B., and C. J. Ammon (2004), *Computer Programs in Seismology: Surface Waves, Receiver Functions and Crustal Structure*, Saint Louis Univ., St. Louis, Mo.
- Horvath, P., G. V. Latham, Y. Nakamura, and H. J. Dorman (1980), Lunar near-surface shear wave velocities at the Apollo landing sites as inferred from spectral amplitude ratios, *J. Geophys. Res.*, *85*, 6572–6578.
- Khan, A., and K. Mosegaard (2002), An inquiry into the lunar interior: A nonlinear inversion of the Apollo lunar seismic data, *J. Geophys. Res.*, *107*(E6), 5036, doi:10.1029/2001JE001658.
- Kovach, R. L., J. S. Watkins, and P. Talwani (1973), Lunar seismic profiling experiment, in *Apollo 17 Preliminary Science Report, NASA Spec. Publ., SP-330*, 12 pp.
- Langseth, M. G., S. J. Keihm, and J. L. Chute (1973), Heat flow experiment, in *Apollo 17 Preliminary Science Report, NASA Spec. Publ., SP-330*, 24 pp.
- Larose, E., A. Derode, M. Campillo, and M. Fink (2004), Imaging from one-bit correlations of wideband diffuse wave fields, *J. Appl. Phys.*, *95*, 8393–8399.
- Latham, G., M. Ewing, J. Dorman, Y. Nakamura, F. Press, N. Toksoz, G. Sutton, F. Duennebier, and D. Lammlin (1973), Lunar structure and dynamics—Results from the Apollo passive seismic experiment, *Moon*, *7*, 396–420.
- Lobkis, O. I., and R. L. Weaver (2001), On the emergence of the Green functions in the correlations of a diffuse field, *J. Acoust. Soc. Am.*, *110*, 3011–3017.
- Lognonné, P., et al. (2000), The NetLander very broad band seismometer, *Planet. Space Sci.*, *48*, 1289–1302.
- Lognonné, P., J. Gagnepain-Beyneix, and H. Chenet (2003), A new seismic model of the Moon: Implications for structure, thermal evolution and formation of the Moon, *Earth Planet. Sci. Lett.*, *211*, 27–44.
- Nakamura, Y., G. V. Latham, and H. J. Dorman (1982), Apollo lunar seismic experiment—Final summary, *Proc. Lunar Planet. Sci. Conf. 13th*, Part 1, *J. Geophys. Res.*, *87*, suppl., A117–A123.
- Paul, A., M. Campillo, L. Margerin, E. Larose, and A. Derode (2005), Empirical synthesis of time-asymmetrical Green functions from the correlation of coda waves, *J. Geophys. Res.*, *110*, B08302, doi:10.1029/2004JB003521.
- Rhie, J., and B. Romanowicz (2004), Excitation of Earth's continuous free oscillations by atmosphere-ocean-seafloor coupling, *Nature*, *431*, 552–556.
- Roux, P., W. A. Kuperman, and the NPAL Group (2004), Extracting coherent wavefronts from acoustic ambient noise in the ocean, *J. Acoust. Soc. Am.*, *116*, 1995–2003.
- Sabra, K. G., P. Gerstoft, P. Roux, W. A. Kuperman, and M. C. Fehler (2005), Surface wave tomography from microseisms in Southern California, *Geophys. Res. Lett.*, *32*, L14311, doi:10.1029/2005GL023155.
- Shapiro, N. M., and M. Campillo (2004), Emergence of broadband Rayleigh waves from correlations of the ambient seismic noise, *Geophys. Res. Lett.*, *31*, L07614, doi:10.1029/2004GL019491.
- Shapiro, N. M., M. Campillo, L. Stehly, and M. H. Ritzwoller (2005), High resolution surface wave tomography from ambient seismic noise, *Science*, *307*, 1615–1618.
- Toksoz, M., A. Dainty, S. Solomon, and K. Anderson (1974), Structure of the Moon, *Rev. Geophys.*, *12*, 539–567.
- van Tiggelen, B. A. (2003), Green function retrieval and time reversal in a disordered world, *Phys. Rev. Lett.*, *91*, doi:10.1103/PhysRevLett.91.243904.
- Weaver, R. L., and O. I. Lobkis (2001), Ultrasonics without a source: Thermal fluctuation correlations at MHz frequencies, *Phys. Rev. Lett.*, *87*, doi:10.1103/PhysRevLett.87.134301.

M. Campillo and E. Larose, LGIT, Université Joseph Fourier, CNRS, UMR 5559, BP53, F-38041 Grenoble Cedex, France. (eric.larose@ujf-grenoble.fr)

A. Khan, Niels Bohr Institute, University of Copenhagen, Juliane Maries Vej 30, DK-2100 Copenhagen Oe, Denmark.

Y. Nakamura, Institute for Geophysics, John A. and Katherine G. Jackson School of Geosciences, University of Texas at Austin, Austin, Texas, USA.